Brevicidine, a bacterial non-ribosomally produced cyclic antimicrobial lipopeptide with a unique *modus operandi*

Xinghong Zhao[a,b,c,1,*], Xinyi Zhong[a,1], Hongping Wan[c,1], Lu Liu[a], Xu Song[a], Yuanfeng Zou[a], Lixia Li[a], Renyong Jia[c], Juchun Lin[a], Huaqiao Tang[a], Gang Ye[a], Jianqing Yang[d], Shan Zhao[c], Yifei Lang[c], Zhongqiong Yin[a,*], Oscar P. Kuipers[b]

[a] Lab for Sustainble Antimicrobials, Department of Pharmacy, Sichuan Agricultural University, Chengdu, 611130, China.

[b] Department of Molecular Genetics, Groningen Biomolecular Sciences and Biotechnology Institute, University of Groningen, Groningen, 9747 AG, The Netherlands.

[c] Key Laboratory of Animal Disease and Human Health of Sichuan Province, Sichuan Agricultural University, Chengdu, 611130, China.

[d] State Key Laboratory of Crop Gene Exploration and Utilization in Southwest China, Sichuan Agricultural University at Wenjiang, Chengdu, Sichuan 611130, China

[1] These authors contributed equally to this work.

* Correspondence: xinghong.zhao@sicau.edu.cn; yinzhongq@163.com

Abstract

Due to the accelerated appearance of antibiotic-resistant (AMR) pathogens in clinical infections, new first-in-class antibiotics, operating via novel modes of action, are desperately-needed. Brevicidine, a bacterial non-ribosomally produced cyclic lipopeptide, has shown potent and selective antimicrobial activity against Gram-negative pathogens. However, before our investigations, little was known about how brevicidine exerts its potent bactericidal effect against Gram-negative pathogens. In this study, we find that brevicidine has potent antimicrobial activity against AMR *Enterobacteriaceae* pathogens, with a MIC value ranging between 0.5μM (0.8mg/L) and 2μM (3.0mg/L). In addition, brevicidine showed potent anti-biofilm activity against the *Enterobacteriaceae* pathogens, with same 100% inhibition and 100% eradication concentration of 4μM (6.1mg/L). Further mechanistic studies showed that brevicidine exerts its potent bactericidal activity via interacting with lipopolysaccharide in the outer membrane, targeting phosphatidylglycerol and cardiolipin in the inner membrane, and dissipating the proton motive force of bacteria. This results in metabolic perturbation, including inhibition of adenosine triphosphate synthesis, inhibits the dehydrogenation of nicotinamide adenine dinucleotides, accumulation of reactive oxygen species in bacteria, and inhibition of protein synthesis. Lastly, brevicidine showed a good therapeutic effect in a mouse peritonitis–sepsis model. Our findings pave the way for further research on clinical applications of brevicidine, to combat the prevalent infections caused by AMR Gram-negative pathogens worldwide.

Keywords: Brevicidine; Antimicrobial resistance; Antimicrobial mechanism; Bacteraemia model; *Escherichia coli*

Introduction

Due to the accelerated appearance of antimicrobial resistance (AMR) in bacterial pathogens, many bacterial infections have become increasingly difficult, or even impossible, to treat with conventional antimicrobials. The O'Neill report on AMR, published in 2014, predicted that deaths attributable to resistant infections will reach 10 million annually by 2050 (1, 2). In addition, due to the COVID-19 pandemic, the AMR situation is getting worse since increasing evidence has emerged that the COVID-19 pandemic also contributes to AMR (2–6). Despite the AMR situation being so urgent, the number of newly approved antimicrobials has been steadily decreasing over the past 20 years, especially those for treating Gram-negative pathogen infections (7–9). Bacteria produce a wealth of non-ribosomally produced peptide (NRP) antimicrobials, including clinically approved antimicrobial cyclic lipopeptides, such as vancomycin, daptomycin, and colistin (10). This shows that the group of cyclic lipopeptides makes up a rich source of molecules able to control pathogenic bacterial infections.

Brevicidine (Bre), a bacterial non-ribosomally produced cyclic lipopeptide, was first isolated from the *Brevibacillus laterosporus* DSM25 in 2018 (11). This cyclic lipopeptide contains 12 amino acids (4-Methyl-Hexanoyl-D-Asn-D-Tyr-D-Trp-D-Orn-Orn-Gly-D-Orn-Trp-Thr-Ile-Gly-Ser) with a 4-Methyl-Hexanoyl chain at its N-terminus and a lactone bond between Thr9 and Ser12 (Fig. 1) (11, 12). In addition, Nathaniel et al reported the total synthetic route of brevicidine in 2022 (13), which makes it more attractive for antibiotic development. Brevicidine displays potent and selective

antimicrobial activity against Gram-negative pathogens, including *Enterobacter cloacae*, *Escherichia coli*, *Pseudomonas aeruginosa*, and *Klebsiella pneumoniae* (11, 14), which are listed as “critical” priority pathogens that need R&D of new antimicrobials by the World Health Organization (WHO) (15). Notably, brevicidine showed no cytotoxicity and hemolytic activity at a relatively high concentration of 128μg/ml (11, 14), indicating brevicidine is a promising antimicrobial candidate. In our previous study, we found that brevicidine dissipated the proton motive force of bacteria. However, before the present investigations, little was known about how brevicidine exerts its potent bactericidal effect against Gram-negative pathogens. In addition, the antimicrobial activity against AMR pathogens and the therapeutic effect *in vivo* of brevicidine still needs to be investigated before it is considered for a clinical trial.

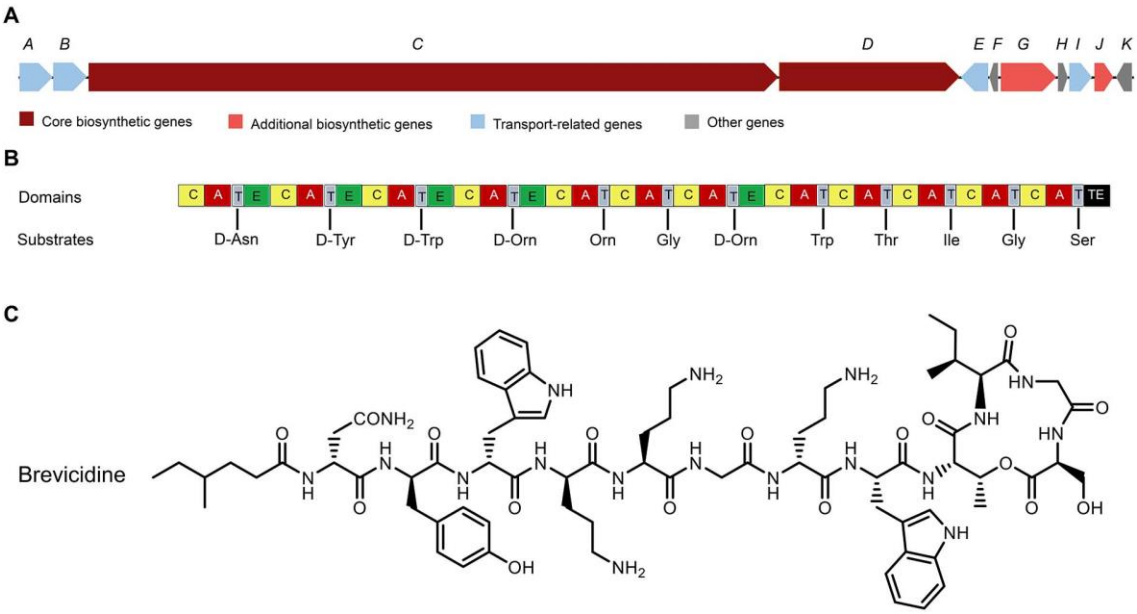

Fig. 1. The structure of brevicidine and the predicted biosynthetic gene cluster (14)**. A**, The non-ribosomal peptide synthetases genes harbored by the *Brevibacillus laterosporus* DSM 25 genome; **B**, the catalytic domains encoded by the gene cluster, and the substrates incorporated by the respective modules. Domains: A, adenylation; T, thiolation; C, condensation; E, epimerization; TE, thioesterase; **C**, the structure of brevicidine.

82 In this study, we aimed to identify the precise molecular mechanism of action by
83 which brevicidine kills Gram-negative pathogens. Moreover, the anti-biofilm activity
84 against *E. coli*, the antimicrobial activity against AMR *Enterobacteriaceae*, and the *in*
85 *vivo* therapeutic effect of brevicidine were also investigated. The results showed that
86 brevicidine exerts its potent bactericidal effect by interacting with lipopolysaccharide
87 (LPS) in the outer membrane as well as targeting phosphatidylglycerol (PG) and
88 cardiolipin (CL) in the inner membrane, and subsequently disrupting the proton
89 motive force of Gram-negative pathogens. This leads to adenosine triphosphate (ATP)
90 synthesis inhibition, nicotinamide adenine dinucleotide (NADH) and reactive oxygen
91 species (ROS) accumulation, and bacteria death. In addition, brevicidine showed
92 potent antimicrobial activity against AMR Gram-negative pathogens and good
93 anti-biofilm activity against Gram-negative pathogen. Notably, brevicidine showed a
94 good therapeutic effect in an *E. coli*-induced mouse peritonitis–sepsis model. These
95 results will pave the way for further research on the clinical applications of
96 brevicidine.

97 Results and Discussion

98 Brevicidine shows potent antimicrobial activity against 99 antibiotic-resistant (AMR) *Enterobacteriaceae* pathogens

100 The antimicrobial activity of brevicidine against AMR *Enterobacteriaceae* pathogens
101 was measured by a MIC assay. The results show that brevicidine has potent
102 antimicrobial activity, with a MIC value of 0.5μM (0.8mg/L) to 2μM (3.0mg/L) (Table
103 1), against *Enterobacteriaceae* pathogens, including the tested colistin-resistant

104 strains and multidrug-resistant strains (16). These results indicate that brevicidine has
105 no cross-resistance with colistin, ampicilin, ceftriaxone, cefotaxime, aztreonam,
106 gentamicin, ofloxacin, amoxicillin, streptomycin, lincomycin, doxycycline, or
107 ciprofloxacin, which makes it a more attractive antimicrobial candidate for treating
108 AMR Gram-negative pathogen infections.

109 **Table 1** MIC values of brevicidine against *Enterobacteriaceae* bacterial pathogens.

Microorganism	**MIC [μM (mg/L)]**			
	Brevicidine	**Colistin**	**Amikacin**	**Ampicilin**
Escherichia coli ATCC25922	0.5 (0.8)	2 (2.3)	2 (1.2)	8 (2.8)
Escherichia coli CVCC3749	1 (1.5)	2 (2.3)	2 (1.2)	> 256 (89)
Escherichia coli B2[a]	1 (1.5)	8 (9.2)	32 (19)	> 256 (89)
Escherichia coli 16QD [a]	1 (1.5)	8 (9.2)	8 (4.7)	> 256 (89)
Escherichia coli EPZC17-45[b]	1 (1.5)	2 (2.3)	4 (2.3)	> 256 (89)
Escherichia coli EPZC17-22[b]	1 (1.5)	1 (1.6)	2 (1.2)	> 256 (89)
Escherichia coli E21-5[b]	0.5 (0.8)	2 (2.3)	2 (1.2)	> 256 (89)
Escherichia coli E21-71[b]	0.5 (0.8)	4 (4.6)	4 (2.3)	> 256 (89)
Escherichia coli E21-75[b]	0.5 (0.8)	2 (2.3)	8 (4.7)	> 256 (89)
Escherichia coli E21-107[b]	0.5 (0.8)	1 (1.6)	4 (2.3)	> 256 (89)
Enterobacter cloacae LMG02783[c]	1 (1.5)	> 64 (74)	8 (4.7)	> 256 (89)
Klebsiella pneumoniae LMG20218	2 (3.0)	2 (2.3)	4 (2.3)	> 256 (89)
Staphylococcus aureus ATCC 43300[d]	32 (48.6)	32 (37)	4 (2.3)	16 (5.6)
Enterococcus faecium LMG16003[e]	> 32 (48.6)	> 32 (37)	256 (150)	2 (0.7)

110 [a]*Escherichia coli* carrying mcr-1, blaNDM-5, mdfA genes, etc., which is resistant against colistin,
111 carbapenems, rifampin, etc. [b] *Escherichia coli* (clinical isolation) carrying multidrug resistance
112 genes, *Escherichia coli* EPZC17-45, resistant to ampicilin, ceftriaxone, cefotaxime, aztreonam,
113 gentamicin, doxycycline, and ciprofloxacin; *Escherichia coli* EPZC17-22, resistant to ampicilin,
114 ceftriaxone, cefotaxime, aztreonam, gentamicin, doxycycline, and ciprofloxacin; *Escherichia coli*
115 E21-5, resistant to ampicilin, amoxicillin, ceftriaxone, gentamicin, cefotaxime, streptomycin,
116 doxycycline; *Escherichia coli* E21-71, resistant to ampicilin, amoxicillin, ceftriaxone, cefotaxime,
117 doxycycline, and ciprofloxacin, and ofloxacin; *Escherichia coli* E21-75, resistant to ampicilin,
118 amoxicillin, ceftriaxone, cefotaxime, doxycycline, ofloxacin, and ciprofloxacin; *Escherichia coli*
119 E21-107, resistant to ampicilin, amoxicillin, ceftriaxone, gentamicin, cefotaxime, streptomycin,
120 doxycycline, and lincomycin. [c]*Enterobacter cloacae* carrying mcr-9 gene, which is a potent
121 colistin-resistant gene. [d] *Staphylococcus aureus* resistant to oxacillin and methicillin. [e]
122 *Enterococcus faecalis* resistant to vancomycin.

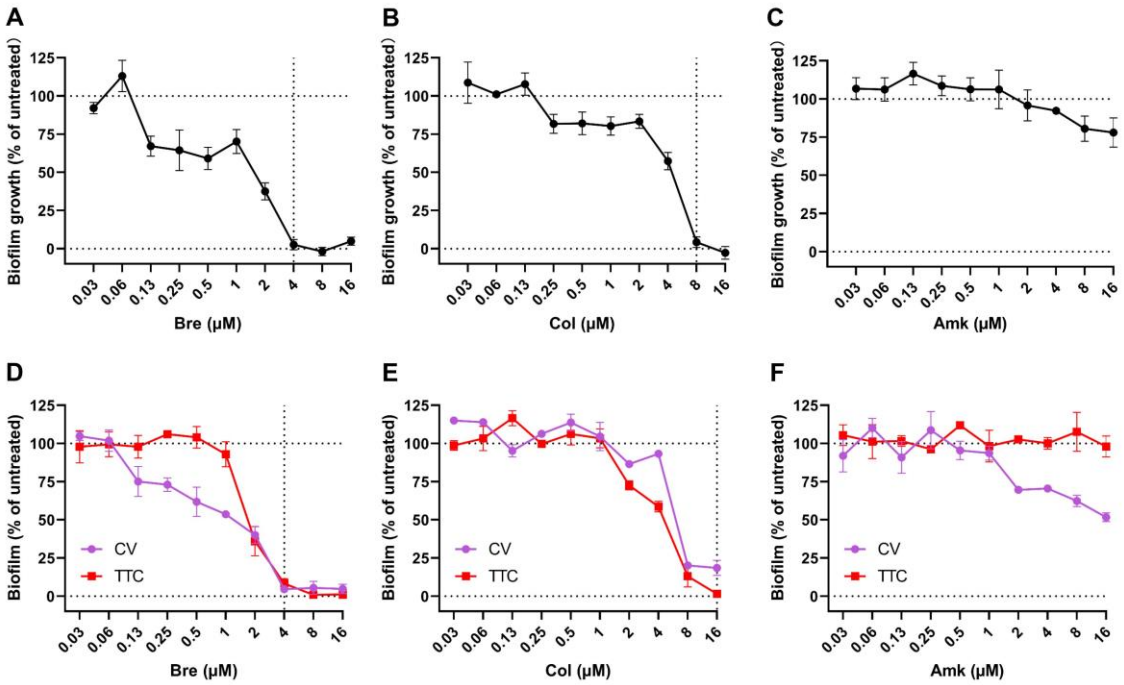

Fig. 2. Brevicidine showed potent anti-biofilm activity against *E. coli* O101. A, Biofilm inhibition of various antimicrobials (brevicidine, colistin, and amikacin) versus *E. coli* O101. Biofilm inhibition was assessed by incubating the antimicrobials with bacteria in growth media for 24 h, discarding the growth media and staining the adhered biomass with CV. The percentage of biofilm inhibition is reported relative to untreated bacteria (defined as 100%) and sterility control wells (defined as 0%). All data were presented as means ± Standard Deviation. **B**, Biofilm eradication assay results for various antimicrobials (brevicidine, colistin, and amikacin) versus *E. coli* O101. Biofilm biomass, quantified based on CV staining, is indicated in pink. Biofilm metabolism, quantified based on TTC metabolism, is indicated in red. All data were presented as means ± Standard Deviation.

Brevicidine shows potent anti-biofilm activity against *E. coli*

Bacterial biofilm formation could increase the resistance of pathogens to conventional antimicrobials, which could decrease the therapeutic effect of antimicrobials (17, 18). Therefore, the anti-biofilm activity of antimicrobials plays a vital role in their therapeutic effect on biofilm-formation bacterial pathogen infections. In this study, the anti-biofilm activity of brevicidine against *E. coli* was evaluated according to the protocol described previously (19). Colistin (Col) was used as an anti-biofilm antimicrobial control, while amikacin (Amk) was used as a control

142 antimicrobial without anti-biofilm activity. The results show that brevicidine has
143 potent anti-biofilm activity against *E. coli*, with the same 100% inhibition and
144 eradication concentration of 4μM (6.1 mg/L), which is better than the anti-biofilm
145 activity of colistin against *E. coli* (Fig. 2). These results demonstrate that brevicidine
146 shows high potential for the development of therapeutic antimicrobial.

147 Brevicidine disrupts the electron transport chain of Gram-negative 148 bacteria

149 In previous studies, brevicidine had shown bacterial lytic activity at a concentration
150 of 10×MIC (11, 14). However, it did not disrupt the membrane at a concentration of
151 2×MIC, evidenced by an atomic force microscopy assay. Therefore, the authors
152 suggested that a more in-depth mechanism study is needed to characterize the
153 targets as well as the membrane disruption effect of brevicidine (11). In our previous
154 study, we found that brevicidine, at a concentration of 1×MIC, could dissipate the
155 proton motive force of *E. coli* , evidence by a $DiSC_3(5)$ assay (14). However, before our
156 investigations, little is known about the molecular mechanism of brevicidine on
157 gram-negative bacteria. In this study, to investigate the killing capacity of brevicidine
158 at concentrations of low MIC values, 4×MIC, 2×MIC, and 1×MIC, a time-killing assay
159 was performed as the previously described method (20, 21). Brevicidine quickly
160 decreased the population of *E. coli* at a concentration of 4×MIC, which killed all of
161 the tested bacteria in 1h. Interestingly, the population of *E. coli* did not decrease
162 under the treatment of brevicidine at concentrations of 2×MIC and 1×MIC within
163 30min (Fig. 3A). These results indicate that brevicidine has different modes of action

164 between high and low MIC concentrations; it shows bacterial lytic activity at
165 concentrations of 4-fold to 10-fold MIC, while it does not disrupt the membrane at
166 concentrations of 1-fold to 2-fold MIC (11, 14). The atomic force microscopy, which
167 was used in the previous study (11), is not a common technique for investigating the
168 membrane effect of antimicrobials because of its low resolution. Therefore, in this
169 study, we performed several fluorescent probe assays, scanning electron microscopy
170 (SEM) assay, and transmission electron microscopy (TEM) assay to get insight into the
171 effect of brevicidine, at low MIC level concentration, on the Gram-negative bacterial
172 membrane.
173 The effect of brevicidine on the membrane integrity of Gram-negative bacteria was
174 investigated by using the fluorescent probes N-Phenyl-1-naphthylamine (NPN) and
175 propidium iodide (PI). NPN is an outer-membrane barrier permeant fluorescent
176 probe (22). If the outer membrane is disrupted, the fluorescent probe can enter,
177 reaching the phospholipid layer and resulting in a significant increase of fluorescence.
178 The fluorescent probe PI is permeant to membrane intact bacteria, and the
179 disruption of membrane integrity can lead to a prominent increase in fluorescence
180 (20). There was no fluorescence increase observed for both brevicidine-treated
181 NPN-containing cell suspensions and brevicidine-treated PI-containing cell
182 suspensions (Fig. 3 B and C), indicating brevicidine does not disrupt the membrane
183 integrity at concentrations of 2×MIC, 1×MIC, and 0.5×MIC.

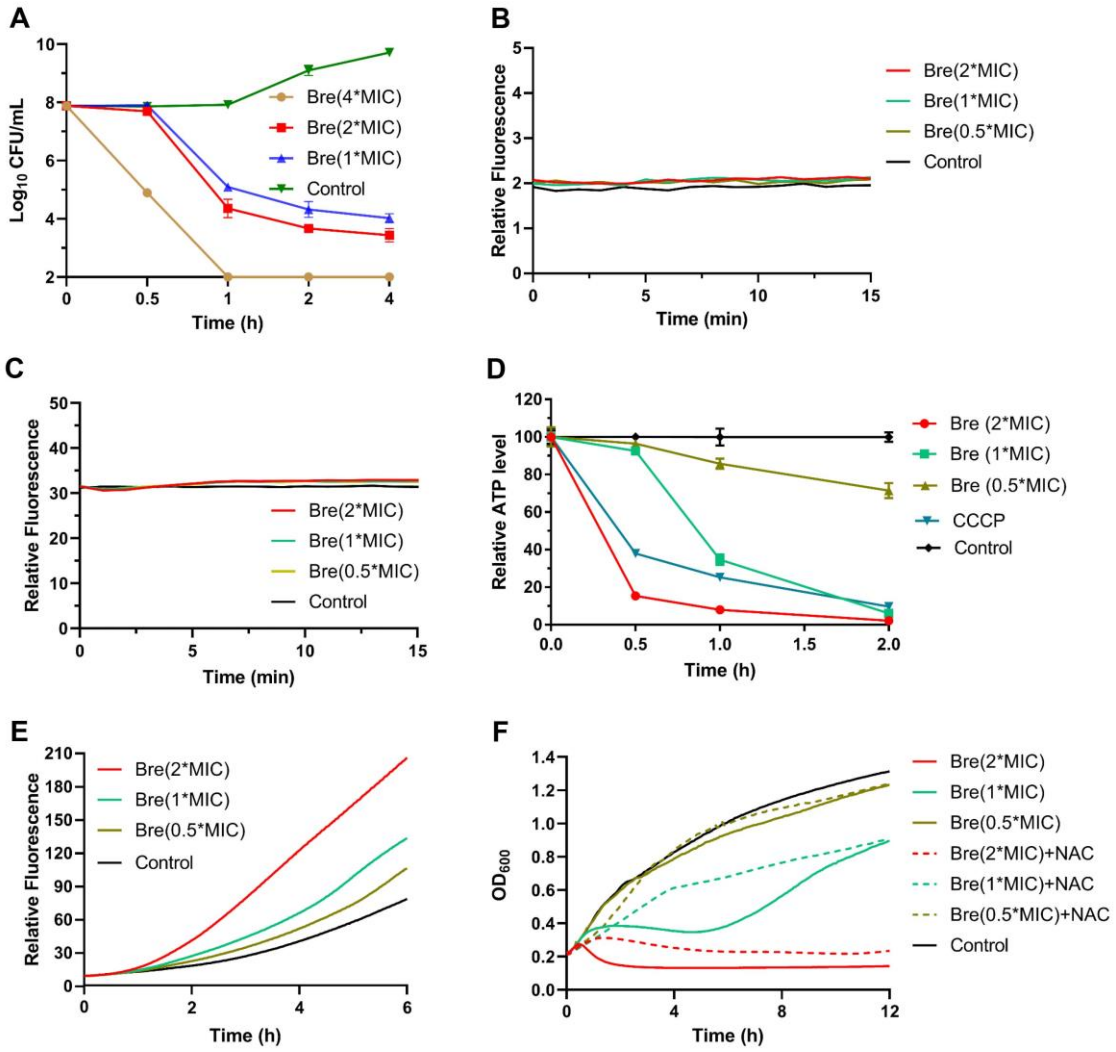

Fig. 3. Brevicidine kills Gram-negative bacteria via dissipating their electron transport chain. A, time-killing curves of brevicidine at concentrations of 4×MIC, 2×MIC, and 1×MIC against *E. coli* O101. **B**, *E. coli* O101 cells pretreated with propidium iodide were exposed to antimicrobial peptides brevicidine at concentrations of 2×MIC, 1×MIC, and 0.5×MIC, and the extent of membrane leakage was visualized as an increase in fluorescence. **C**, NPN fluorescence in *E. coli* O101 cells upon exposure to brevicidine at concentrations of 2×MIC, 1×MIC, and 0.5×MIC. Representative examples from three technical replicates are shown. **D**, ATP concentration of *E. coli* O101 cells treated with brevicidine at concentrations of 2×MIC, 1×MIC, and 0.5×MIC. **E**, Total ROS accumulation in *E. coli* O101 cells treated with brevicidine at concentrations of 2×MIC, 1×MIC, and 0.5×MIC. Representative examples from three technical replicates are shown. **F**, Growth curves of *E. coli* O101 exposed to brevicidine at concentrations of 2×MIC, 1×MIC, and 0.5×MIC. Exogenous addition of NAC (6 μM) diminished the bactericidal activity of brevicidine.

Although brevicidine showed no effect on the bacterial membrane integrity, our previous study had shown that brevicidine dissipated the proton motive force of bacteria as some novel antimicrobials do (14, 23, 24). The proton motive force of

200 bacteria is essential for the generation of ATP, which is an essential bioactive
201 compound for live bacteria (25, 26). If the proton motive force of bacteria is
202 dissipated, the process of ATP biosynthesis will be inhibited or even terminated. To
203 confirm that brevicidine can dissipate the proton motive force of bacteria, the ATP
204 levels of brevicidne, at concentrations of 2×MIC, 1×MIC, and 0.5×MIC, treated
205 bacteria were measured by using the BacTiter-Glo Microbial Cell Viability Assay
206 (Promega) kit. The results showed that brevicidine decreased the ATP level of
207 bacteria as expected (Fig. 3D). These results confirmed that brevicidine could
208 dissipate the proton motive force of bacteria, which is one of the mechanisms by
209 which brevicidine acts as a bactericidal antimicrobial.
210 The dissipation of the proton motive force of bacteria can result in an increase in the
211 NADH levels of cells. Indeed, our previous study showed that the dehydrogenation of
212 NADH can be inhibited by the addition of brevicidine (14). Considering the
213 importance of the dehydrogenation of NADH to the electron transport chain of
214 bacteria, we hypothesized that brevicidine treatment could result in the
215 accumulation of ROS and thereafter kills bacteria. Therefore, the ROS levels of
216 bacteria treated with different concentrations of brevicidine were measured by using
217 a commercial kit (Beyotime, catalogue no. S0033S). The results show that brevicidine
218 increases the ROS level of bacteria (Fig. 3E), which is one of the reasons that
219 brevicidine shows bactericidal activity. This was further demonstrated by growth
220 curve assay, which showed that the bactericidal activity of brevicidine was
221 attenuated by the addition of the antioxidant N-Acetyl-L-cysteine (NAC, 6 mM) (Fig.
222 3F). Taking together, these results demonstrate that brevicidine exerts its bactericidal
223 activity via dissipating the proton motive force of bacteria and thereafter inhibits ATP

224 biosynthesis, inhibits the dehydrogenation of NADH, accumulates ROS in bacteria,

225 and results in bacteria death.

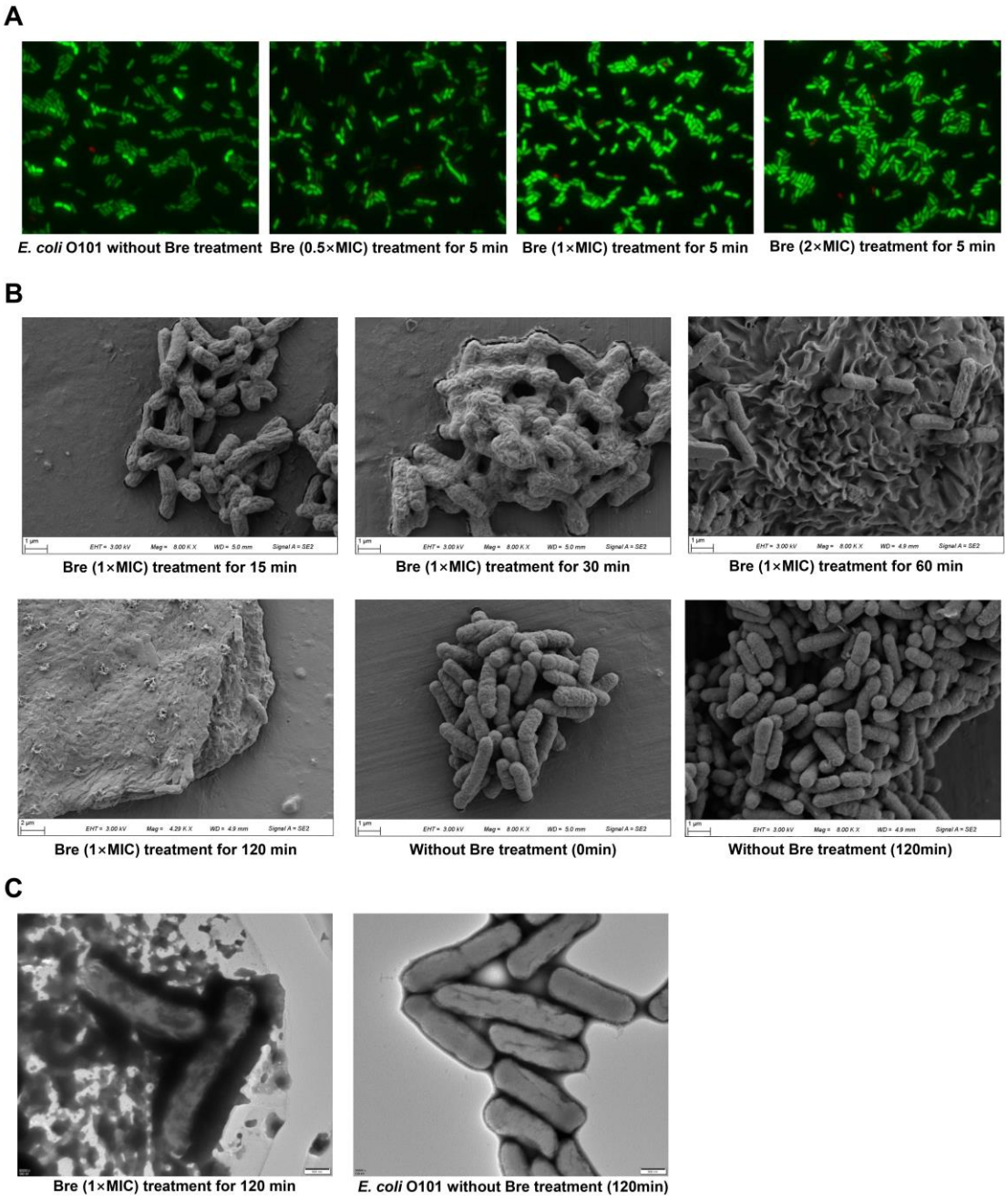

226

227 **Fig. 4. The morphology analysis of *E. coli* O101 under the treatment of brevicidine. A**,
228 Fluorescence microscopy images of *E. coli* O101 cells, which were challenged with brevicidine at
229 concentrations of 2× MIC, 1× MIC, and 0.5× MIC for 5min. Green denotes a cell with an intact
230 membrane, whereas red denotes a cell with a compromised membrane. **B**, SEM image of *E. coli*
231 O101 cells after treatment with brevicidine at a concentration of 1× MIC for 15min, 30min, 60min,
232 and 120min. **C**, TEM image of *E. coli* O101 cells after treatment with brevicidine at a
233 concentration of 1× MIC for 120min.

234

235 To investigate the effect of brevicidine on the cell membrane in intuitive ways, we
236 performed fluorescence microscopy, SEM, and TEM assays. The fluorescence
237 microscopy assay results are consistent with the PI and NPN assays, which
238 demonstrate that brevicidine is not an antimicrobial that kills pathogens by
239 disrupting bacteria membrane integrity (Fig. 4A). Interestingly, after treatment with
240 brevicidine (1×MIC) for 15 min, the bacterial surface fold was observed (Fig. 4B). In
241 addition, after treatment with brevicidine (1×MIC) for 120 min, most of the bacteria
242 were broken, evidenced by SEM and TEM images (Fig. 4 B and C). These results are
243 consistent with the results of time killing assay (Fig. 3A), which showed that
244 brevicidine started to kill bacteria after 30min treatments.

245 Brevicidine targets the membrane components LPS, PG, and CL

246 As brevicidine dissipates the proton motive force of bacteria, we hypothesized that
247 brevicidine could target the component of the bacterial inner membrane. In addition,
248 previous studies showed that brevicidine could interact with LPS (27, 28). To get an
249 insight into the potential target, an agar diffusion assay was performed to investigate
250 if there is an interaction between brevicidine and LPS (outer membrane component),
251 phosphatidylethanolamine (PE, outer and inner membrane component), PG (inner
252 membrane component), or CL (inner membrane component) (29, 30). The main
253 component of mammalian cellular membrane phosphatidylcholine (PC) was used as
254 a control. The results show that the addition of PC or PE did not attenuate the
255 antimicrobial activity of brevicidine (Fig. 5A). In contrast, the antimicrobial activity
256 was completely abolished by the addition of LPS, PG, or CL (Fig. 5A).

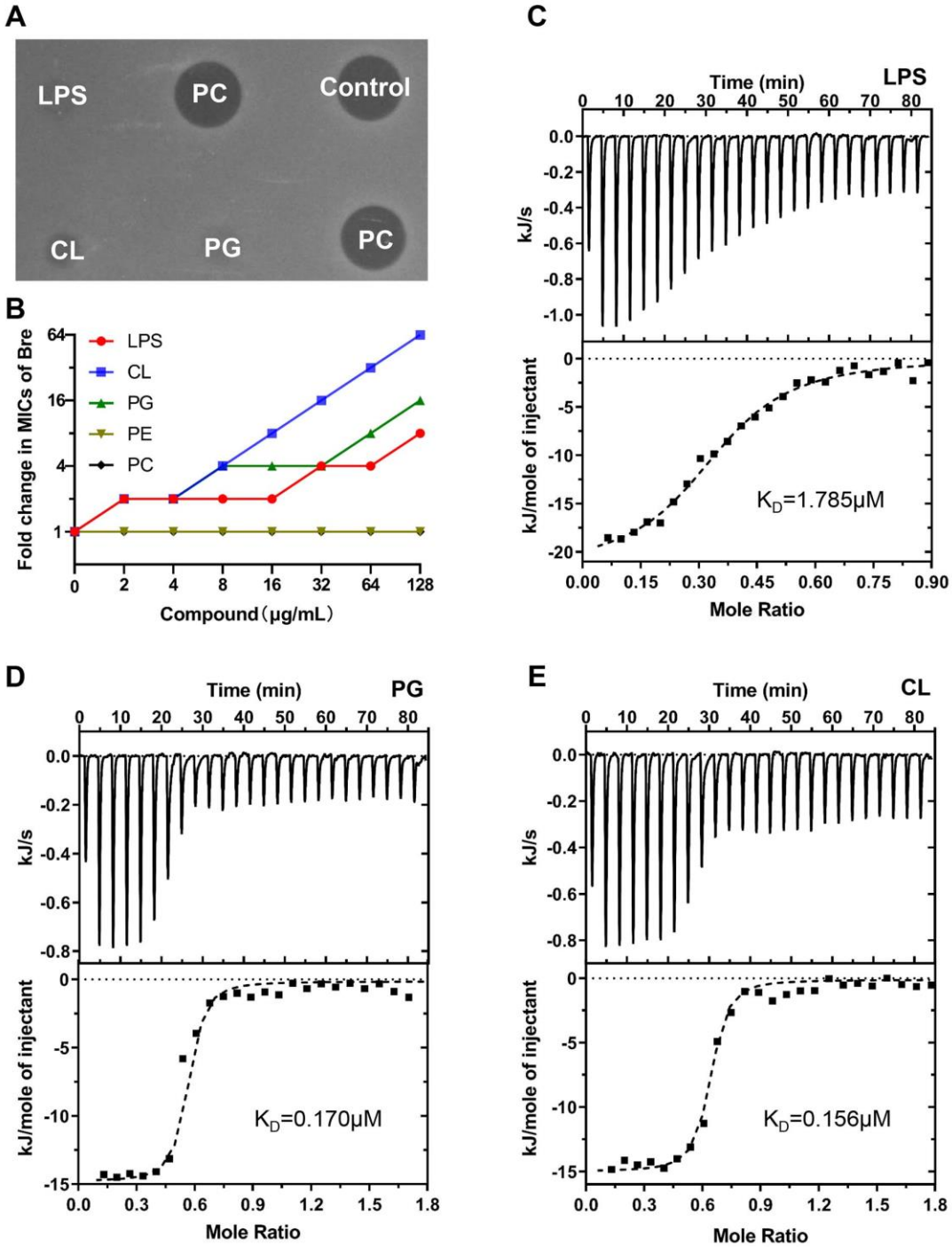

Fig. 5. Brevicidine targets the membrane components LPS, PG, and CL. A, Exogenous addition of LPS, PG, or CL abolishes the antibacterial activity of brevicidine against *E. coli* O101. Inhibition zones of the mixtures of 1 nmol of brevicidine and 4 mmol of PC, LPS, PE, PG and CL, against *E. coli* O101 for overnight incubation at 37 °C. Representative examples from three technical replicates are shown. **B**, Increased MICs of brevicidine against *E. coli* O101 in the presence of LPS, PG and CL, ranging from 0 μg/ml to 128 μg/ml, based on MIC assays. Representative examples from three technical replicates are shown. **C**, ITC analysis of the interaction between brevicidine and LPS. **D**, ITC analysis of the interaction between brevicidine and PG. **E**, ITC analysis of the interaction between brevicidine and CL. The K_D values of brevicidine to LPS, PG and CL were calculated using the Nano Analyze Software (Waters LLC).

268 Subsequently, to investigate the dose-dependent effect of LPS, PG, or CL on the
269 antimicrobial activity of brevicidine, a MIC assay was performed with different
270 concentrations of LPS, PG, CL, PC, or PE. The MIC value of brevicidine had no changes
271 with the addition of PC and PE, suggesting there is no interaction between
272 brevicidine and PE (or PC) (Fig. 5B). This could explain why brevicidine targets the
273 Gram-negative bacteria but has low cytotoxicity to mammalian cells (11, 14). LPS, PG,
274 and CL decreased the antimicrobial activity of brevicidine in a dose-dependent
275 manner, and the MIC value of brevicidine increased 8-fold, 16-fold, and 64-fold by
276 the addition of 128μg/ml of LPS, PG, and CL, respectively (Fig. 5B). These results
277 indicate that brevicidine could bind to the cell membrane components LPS, PG, and
278 CL.
279 To gain an insight into the interaction between brevicidine and LPS, PG, or CL, an ITC
280 measurement was performed. The results show that CL and PG showed comparable
281 binding affinity to brevicidine, with K_D values of 0.156 μM and 0.170 Mm (Fig. 5 C
282 and D), respectively. Notably, CL and PG have much stronger (approximately 10-fold
283 stronger) binding affinity to brevicidine than LPS, which has a K_D value of 1.785 μM
284 (Fig. 5E). These results demonstrate that brevicidine has multiple targets on the
285 bacteria, which is good for inhibiting the development of bacterial antibiotic
286 resistance. Together, the observed results demonstrate that brevicidine exerts its
287 bactericidal activity via interacting with LPS in the outer membrane and targeting CL
288 and PG in the inner membrane, and thereafter dissipating the proton motive force of
289 bacteria.

290 **Brevicidine inhibits the oxidative phosphorylation and protein**
291 **synthesis processes of *E. coli***

292 To gain an insight into the antimicrobial mechanism of brevicidine, transcriptome
293 analysis was performed on *E. coli* treated with or without brevicidine at a
294 concentration of 0.5μM (0.8 mg/L). The whole distribution of differentially expressed
295 genes (DEGs) is shown in Fig. 6A. When padj value<0.05 and log2(FoldChange)>0,
296 among 4622 genes, 587 were upregulated and 622 were downregulated, and 3413
297 genes were not significantly changed (Fig. 6A). Subsequently, Kyoto Encyclopedia of
298 Genes and Genomes (KEGG) enrichment analysis was performed on the genes that
299 had significantly expression changes. The results showed that ribosome, oxidative
300 phosphorylation, and aminoacyl-tRNA biosynthesis pathways were significantly (padj
301 value<0.05) affected by brevicidine treatment (Fig. 6B). After *E. coli* exposure to
302 brevicidine for 1h oxidative phosphorylation related genes including ATP synthase,
303 NADH-quinone oxidoreductase, and cytochrome oxidase were significantly
304 downregulated (Fig. 6C). This change would contribute to the lower level of ATP,
305 higher level of NADH and ROS of the brevicidine treated cells. The downregulated
306 tRNA ligase and ribosome synthesis metabolism indicate that the protein synthesis
307 process was inhibited by brevicidine treatment.

308

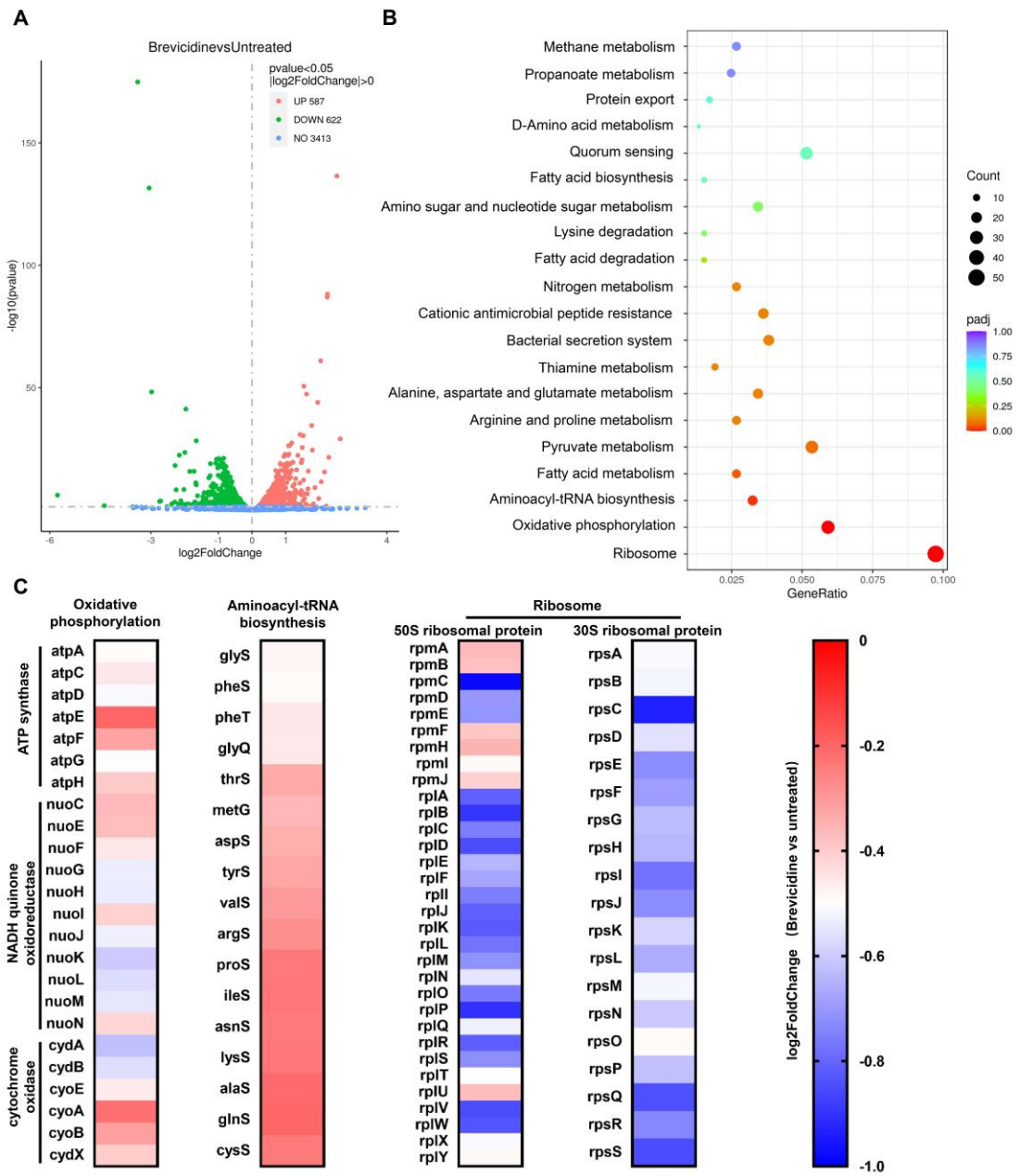

Fig. 6. Transcriptome analysis of *E. coli* O101 under the treatment of brevicidine [0.5 μM (0.8 mg/L)] for 1 h. A, The volcano map of DEGs. The abscissa represents the multiple changes of gene expression between brevicidine treated and untreated *E. coli* O101; the ordinate represents the statistical significance of the change of gene expression (pvalue<0.05 |log2FoldChange|>0). **B**, Scatter plot of KEGG pathway enrichment analysis of DEGs (Brevicidine vs untreated). The vertical axis represents the KEGG enrichment analysis pathway name, and the horizontal axis represents the gene ratio of the genes in the pathway. The size of the dots indicates the number of DEGs in the pathway, and the color of the dots corresponds to different padj value ranges. **C**, Genes involved in oxidative phosphorylation, ribosome, and aminoacyl-tRNA biosynthesis were identified as significantly different between the treatment of brevicidine and untreated, with pvalue values <0.05 and log2FoldChange <0 in expression level. All genes that had significantly changes were down-regulated in oxidative phosphorylation, ribosome, and aminoacyl-tRNA biosynthesis pathways. All data are presented as means (n= 3 biological replicates).

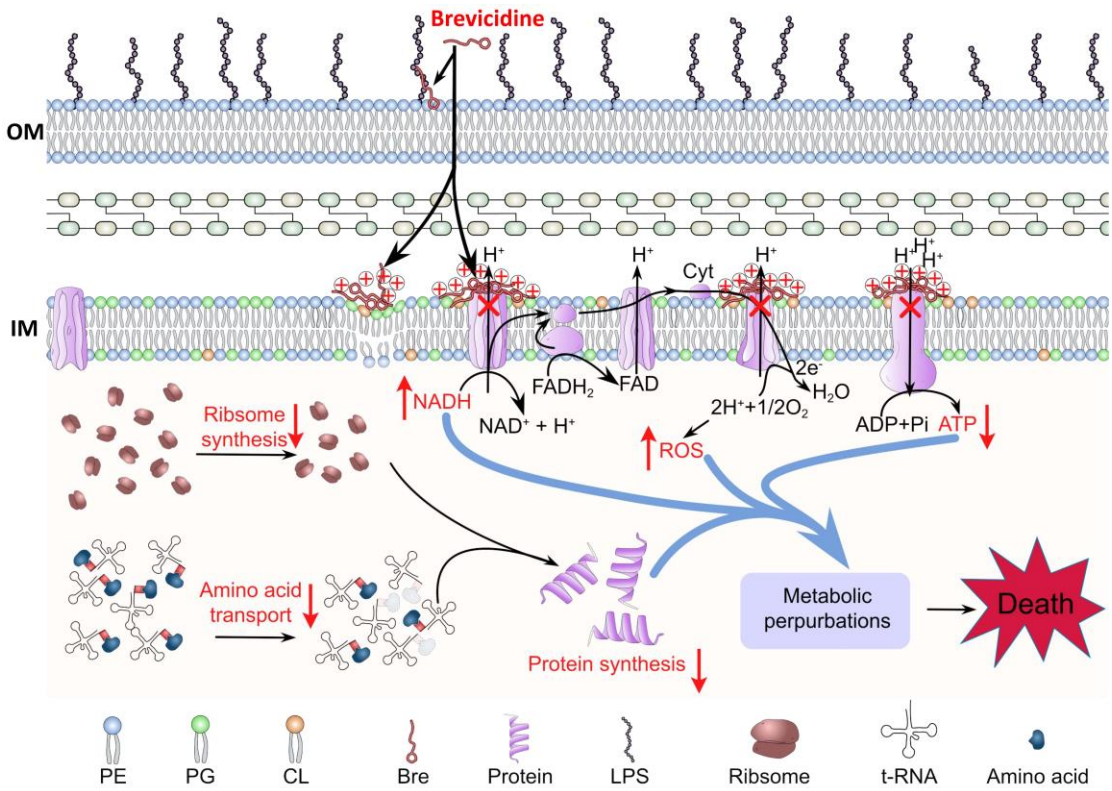

Fig. 7. Scheme of the proposed mechanism of action brevicidine against *E. coli*. Brevicidine exerts its bactericidal activity via interacting with LPS in the outer membrane (OM) and targeting CL and PG in the inner membrane (IM), which could make a positive potential surround the outside surface of inner membrane (Note: no evidence shows brevicidine directly interacts with these channel proteins), and thereafter dissipating the proton motive force of the bacteria. This results in metabolic perturbation, including decreases in the intracellular ATP level, inhibits the dehydrogenation of NADH and accumulates ROS in bacteria. In addition, transcriptome analysis results showed that brevicidine inhibits the synthesis of t-RNA ligase (essential for amino acid transport) and ribosome protein synthesis, which can result in protein synthesis inhibition. All these actions together lead to the death of Gram-negative pathogens.

Collectively, our findings demonstrate that brevicidine exerts its bactericidal activity via interacting with LPS in the outer membrane and targeting CL and PG in the inner membrane, and thereafter dissipation of the proton motive force of bacteria. This can result in metabolic perturbation, including inhibits ATP biosynthesis, inhibits the dehydrogenation of NADH, accumulates ROS in bacteria, and inhibits protein synthesis (Fig. 7).

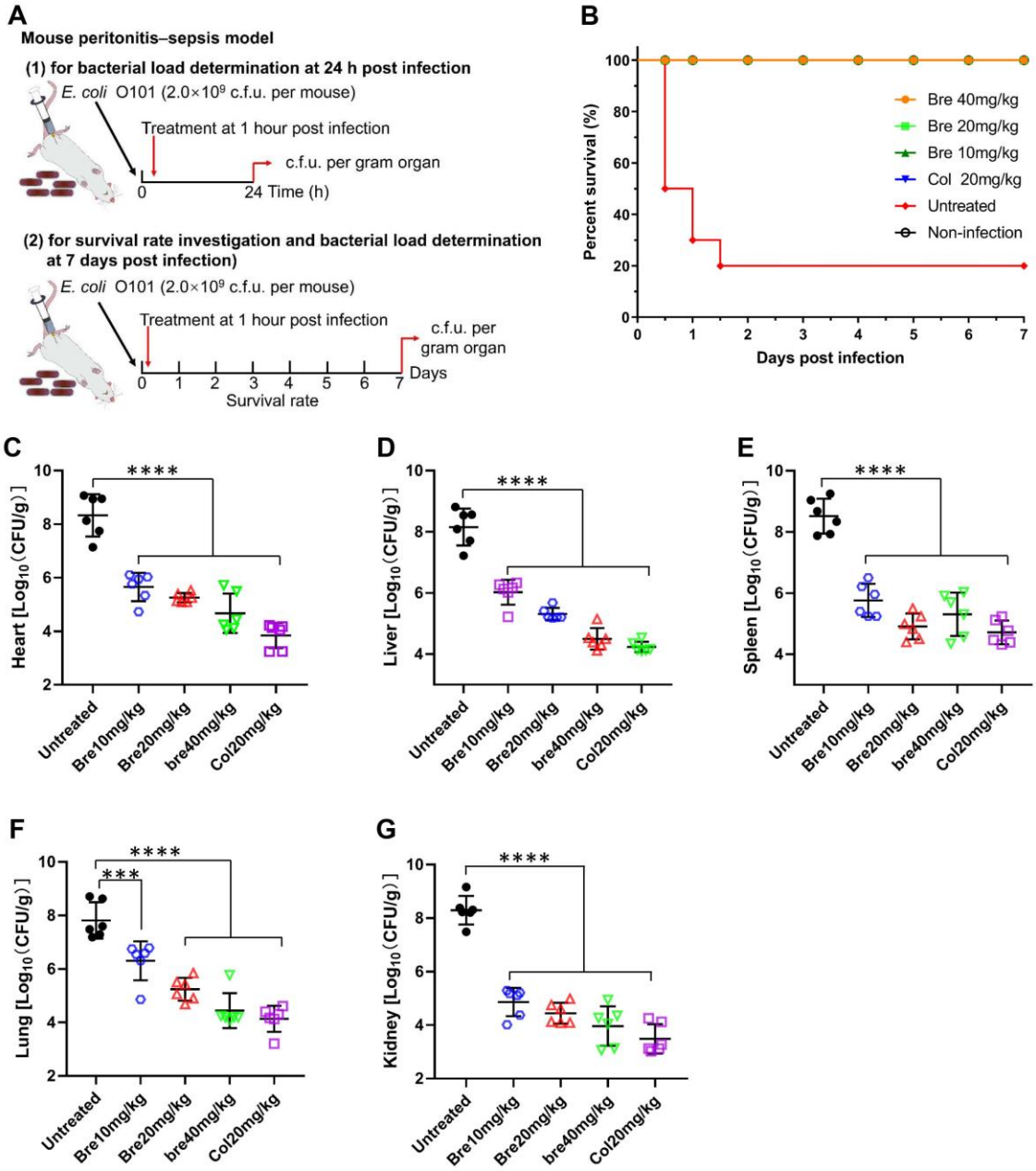

Fig. 8. Brevicidine showed a good therapeutic effect in a mouse peritonitis–sepsis model. A, Scheme of the experimental protocol for the mouse peritonitis–sepsis model. **B**, Survival rates of mice in the mouse peritonitis–sepsis model (n= 10). Increased survival rates of mice over 7 d by a dose that leads to 80% of death of *E. coli* O101 (2.0×10^9 c.f.u.), treated with brevicidine (10 mg per kg, 20 mg per kg, or 40 mg per kg) or with colistin (20 mg per kg). **C to G**, Brevicidine significantly reduced the bacterial load of organs of the peritonitis-sepsis mouse. At 24h post-infection, the survived mice (n = 6) were euthanized by cervical dislocation. Bacterial loads (Log10 CFU per gram of *E. coli* O101) of the heart (**C**), liver (**D**), spleen (**E**), lung (**F**) and kidney (**G**) were counted. All data were presented as means ± Standard Deviation (n = 6). Correlation analyses were evaluated by Pearson r2, ns: ***$p < 0.01$ and ****$p < 0.001$ vs. untreated group.

354 **Brevicidine showed a good therapeutic effect in a mouse**
355 **peritonitis–sepsis model**

356 Given the attractive mode of action and potent antimicrobial and anti-biofilm activity
357 of brevicidine, we investigated its potential as a therapeutic in a mouse
358 peritonitis–sepsis model (Fig. 8A). Mice were infected intraperitoneally with *E. coli* at
359 a dose that leads to 80% of death. At 1h post-infection, brevicidine was introduced at
360 single intravenous doses ranging from 10mg/kg to 40mg/kg. All brevicidine-treated
361 mice were survived (Fig. 8B). Consistently, the bacterial load in different organs of
362 mice significantly reduced under brevicidine treatment in a dose-dependent manner
363 at either 1 or 7 days post-infection (Fig. 8 C-G, and Supplementary Fig. S1). These
364 results are consistent with the previous study, which showed that brevicidine had
365 good antimicrobial activity in a mouse thigh model (11). Together, these findings
366 demonstrate the potential of brevicidine as a novel therapeutic antimicrobial in AMR
367 Gram-negative pathogen infections, in particular, AMR *Enterobacteriaceae* pathogen
368 infections.

369 **Conclusions**

370 AMR poses a major threat to human health around the world; many bacterial
371 infections have become increasingly difficult, or even impossible, to treat with
372 conventional antimicrobials. Therefore, new first-in-class antibiotics, operating via
373 novel modes of action, are desperately-needed. Here, we show that brevicidine has
374 potent antimicrobial activity against AMR *Enterobacteriaceae* pathogens, with a MIC
375 value range of 0.5μM (0.8mg/L) to 2μM (3.0mg/L). In addition, brevicidine showed

376 potent anti-biofilm activity against the *Enterobacteriaceae* pathogens, with the same
377 100% inhibition and eradication concentration of 4μM (6.1mg/L). Mechanistic
378 studies showed that brevicidine exerts its potent bactericidal activity via interacting
379 with LPS in the outer membrane, targeting PG and CL in the inner membrane, and
380 dissipating the proton motive force of bacteria. This results in metabolic perturbation,
381 including inhibition of ATP biosynthesis, inhibition of the dehydrogenation of NADH,
382 accumulation of ROS in bacteria, and inhibition of protein synthesis (Fig. 7). Lastly,
383 brevicidine showed a good therapeutic effect in a mouse peritonitis–sepsis model.
384 Our findings pave the way for further research on clinical applications of brevicidine,
385 to combat the prevalent infections caused by AMR Gram-negative pathogens
386 worldwide.

387 Materials and Methods

388 Ethical approval

389 The animal experiment protocol was approved by the Animal Ethical and welfare
390 Committee of Sichuan Agricultural University [permission number 20220087].

391 Bacterial strains used and growth conditions

392 Bacterial strains used in this study are listed in S1 Table. All bacterial strains were
393 inoculated in LB and incubated at 37°C with aeration at 220 rpm for preparing the
394 overnight cultures.

395 Purification of brevicidine

396 Methods for the purification of brevicidine have been described in detail previously
397 (12). The matrix-assisted laser desorption ionization-time-of-flight mass spectrometry

398 data and high-performance liquid chromatograph trace of purified brevicidine are
399 shown in Supplementary Figs. S2 and S3, which are showing the correct molecular
400 weight and high purity of the purified brevicidine.

401 Minimum inhibitory concentration (MIC) assay

402 MIC values of antimicrobials against the tested bacterial pathogens were determined
403 according to the standard guidelines (31). Briefly, cell concentration was adjusted to
404 approximately 5×10^5 cells per ml in cation-adjusted Mueller-Hinton broth (MHB).
405 Subsequently, antimicrobials were added to the above bacterial cultures at different
406 concentrations. After 24h of incubation at 37°C, the MIC value was defined as the
407 lowest concentration of antimicrobial with no visible growth.

408 For measuring the MIC values of antimicrobials against indicator strains in the
409 presence of cell membrane components, MHB was replaced with MHB containing
410 different concentrations of cell membrane components, and the effect of these two
411 conditions was compared.

412 Biofilm inhibition assay

413 Biofilm inhibition assay was performed according to a previously described protocol
414 (19). Briefly, an overnight culture of *E. coli* O101 was diluted 100-fold in tryptone soy
415 broth (TSB) and incubated at 37 °C with aeration at 220 r.p.m. Bacteria were grown to
416 an OD_{600} of 0.8, and then the concentration of cells was adjusted to an OD_{600} of 0.04
417 in TSB. The cell suspension was added to a 96-well plate, and antimicrobials were
418 added at different final concentrations. After incubation at 37 °C for 24 h, the wells
419 were washed with MiliQ water three times, and the adhered biomasses were stained
420 with 105 µl of a 0.1% crystal violet (CV) (wt/vol) solution. The plate was placed on a

421 low-speed orbital shaker and allowed to stain at room temperature for 30 min.
422 Subsequently, the plate was washed with MiliQ water three times, and then 70%
423 (vol/vol) ethanol was added to the wells (110 µl per well) and incubated for 30 min at
424 room temperature with gentle shaking. The absorbance was measured by using a
425 Thermo Scientific Varioskan™ LUX multimode microplate reader with a wavelength of
426 595 nm. The inhibition rates were calculated by the raw CV absorbance values from
427 each growth condition vs the raw CV absorbance value of normally grown biofilm.
428 Representative examples from three technical replicates are shown.

429 **Biofilm eradication assay**

430 Biofilm eradication assay was performed according to a previously described protocol
431 (19). Briefly, an overnight culture of *E. coli* O101 was diluted 100-fold in tryptone soy
432 broth (TSB) and incubated at 37 °C with aeration at 220 r.p.m. Bacteria were grown to
433 an OD_{600} of 0.8, and then the concentration of cells was adjusted to an OD_{600} of 0.04
434 in TSB. The cell suspension was added to 96-well plates and incubated at 37 °C for 24
435 h. After washing the wells with TSB three times, antimicrobials were added to the
436 wells at different concentrations, and the plates (one for CV staining, the other one
437 for TTC staining) were incubated at 37 °C for 24 h. For measuring the metabolic
438 activity of biofilm, a final concentration of 0.05% TTC was added to wells with
439 antimicrobials. Subsequently, the adhered biomasses were measured as the method
440 described in the biofilm inhibition assay. After washing all the wells of the TTC plate
441 three times with distilled water, dimethyl sulfoxide (DMSO) was added to the wells at
442 205 µl per well. After that, the plate was placed on an orbital shaker rotating at low
443 speed and mixed at room temperature for 30 min. The absorbance of the TTC plate
444 was measured by using a Thermo Scientific Varioskan™ LUX multimode microplate

445 reader with a wavelength of 500 nm. The biofilm eradication (Biomass and
446 metabolism) rate was calculated by the method described in the previous study (19).
447 Representative examples from three technical replicates are shown.

448 Time-dependent killing assay

449 The time-dependent killing assay was performed according to the procedure
450 described previously (20, 21). An overnight culture of *E. coli* O101 was diluted
451 100-fold in MHB and incubated at 37 °C with aeration at 220 r.p.m. Bacteria were
452 grown to an OD of 0.6, and then the concentration of cells was adjusted to 7.6×10^7
453 cells per mL. Bacteria were then challenged with antimicrobials at concentrations of
454 1×MIC, 2×MIC, or 4×MIC in glass culture tubes at 37 °C with aeration at 220 r.p.m.
455 Bacteria not treated with antimicrobials were used as normal growth control. At
456 desired time points, two hundred µl aliquots were taken, centrifuged at 5,000 g for 5
457 min, and resuspended in 200 µl of MHB. Ten-fold serially diluted samples were plated
458 on MHA plates. After incubation at 37 °C for 24 h, colonies were counted, and the
459 colony forming units (c.f.u.) per ml were calculated. Each experiment was performed
460 in triplicate.

461 Membrane integrity assay

462 A fresh culture of *E. coli* O101 was pelleted at 5,000 g for 5 min and washed three
463 times with MHB. The cell density was normalized to an OD_{600} of 0.2, loaded with
464 propidium iodide (final concentration 2.5 µg per ml), and incubated for 5 min in the
465 dark for probe fluorescence to stabilize. After the cell suspension was added to a
466 96-well microplate, brevicidine was added to final concentrations of 2×MIC, 1×MIC,
467 or 0.5×MIC, with the antimicrobials added after ~30 s, and fluorescence was
468 monitored for 15 min. The excitation and emission wavelengths on the fluorescence

469 spectrometer were adjusted to 533 nm and 617 nm, respectively. Representative
470 examples from three technical replicates are shown.

471 Outer membrane permeability assay

472 The integrity of the outer membrane was investigated with the fluorescent probe
473 N-Phenyl-1-naphthylamine (NPN, Aladdin). A fresh culture of *E. coli* O101 was
474 pelleted at 5,000 g for 5 min and washed three times with 10 mM HEPES containing
475 10 mM glucose (GHEPES, pH 7.2). The cell density was normalized to an OD_{600} of 0.2
476 in GHEPES, loaded with NPN (final concentration 30 μM), and incubated for 30 min in
477 the dark for probe fluorescence to stabilize. After the cell suspension (190 μL) was
478 added to a 96-well microplate, brevicidine (10 μL) was added to final concentrations
479 of 2×MIC, 1×MIC, or 0.5×MIC, with the antimicrobials added after ~30 s, and
480 fluorescence was monitored for 15 min. The excitation and emission wavelengths on
481 the fluorescence spectrometer were adjusted to 350 nm and 420 nm, respectively.
482 Representative examples from three technical replicates are shown.

483 Fluorescence microscopy assay

484 This assay was performed according to the procedure described previously (32, 33). *E.*
485 *coli* O101 was grown to an OD_{600} of 0.6 in MHB. The culture was pelleted at 5,000 g
486 for 5 min and washed with MHB three times. After normalization of the cell density
487 to an OD_{600} of 0.2 in MHB, brevicidine was added to a final concentration of 2×MIC,
488 1×MIC or 0.5×MIC. After incubation at 37 °C for 5min, cells were collected by
489 centrifugation. Subsequently, SYTO® 9 and propidium iodide (LIVE/DEAD Baclight
490 Bacterial Viability Kit, Invitrogen) were added to the above cells. After incubation at
491 room temperature for 15 min, cells were washed three times with MHB. Then the
492 cell suspensions were loaded on 1.5 % agarose pads and analyzed by Nikon 80i

493 (Japan) microscope.

494 ATP determination

495 The ATP levels were determined using a BacTiter-Glo Microbial Cell Viability Assay kit
496 (Promega). A fresh culture of *E. coli* O101 was pelleted at 5,000 g for 5 min and
497 washed three times with MHB. The cell density was normalized to an OD_{600} of 0.2,
498 loaded with brevicidine at final concentrations of 2×MIC, 1×MIC, or 0.5×MIC. At
499 desired time points, 100 μl of cell culture were taken out, mixed with 100 μl
500 BacTiter-Glo reagent, and incubated for 5 minutes at room temperature.
501 Luminescence was measured with an Infinite M2000pro Microplate reader (Tecan).
502 CCCP (40 μg/mL) was used as a positive control. The relative ATP levels were
503 calculated using the measured Luminescence values vs the Luminescence value of
504 untreated cells at relative time points.

505 Reactive oxygen species (ROS) measurement

506 The levels of ROS in *E. coli* O101 treated with different concentrations of brevicidine
507 were measured by 10 μM of 2′,7′-dichlorofluorescein diacetate (DCFH-DA), following
508 the manufacturer's instruction (Beyotime, catalogue no. S0033S). Briefly, a fresh
509 culture of *E. coli* O101 was pelleted at 5,000 g for 5 min and washed three times with
510 MHB. The cell density was normalized to an OD_{600} of 1.0, loaded with DCFH-DA at a
511 final concentration of 10 μM, and the mixture incubated at 37 °C for 30 min. After
512 washing with MHB three times, 190 μl of probe-labeled bacterial cells were added to
513 a 96-well plate, and then 10 μl of brevicidine. Fluorescence was recorded by using a
514 Thermo Scientific Varioskan™ LUX multimode microplate reader with the excitation
515 wavelength at 488 nm and the emission wavelength at 525 nm. The antioxidant
516 N-Acetyl-L-cysteine (NAC, 6 mM) was used as a control to neutralize the production

517 of ROS.

518 Scanning electron microscopy (SEM) and transmission electron 519 microscopy (TEM) assays

520 The morphology of 1μM (1.52 mg/L) brevicidne treated *E. coli* O101 was recorded in
521 vacuum on a ZEISS Gemini SEM300 with an acceleration voltage of 3kV. For TEM
522 measurements, samples were prepared by delivering 2μl of 1μM (1.52 mg/L)
523 brevicidine treated *E. coli* O101 suspension to carbon-coated copper grids and dried
524 in a vacuum system. The morphology was obtained under a JEM-2100Plus Electron
525 Microscope using an acceleration voltage of 120kV.

526 Spot-on-lawn assay

527 An overnight cultured *E. coli* O101 was added to 0.7% MHA (w/v, temperature 42 °C)
528 at a final concentration of 0.25% (v/v), and then the mixture was poured onto the
529 plates, with 20 mL for each 15 cm diameter circular plate. Subsequently, a
530 spot-on-lawn assay was used to analyze the antimicrobial activity of brevicidine in
531 the presence of cell membrane components (20). In short, 20 μL brevicidine (50 μM)
532 containing 200 μM lipopolysaccharides (LPS, from Escherichia coli 055:B5, Solarbio,
533 catalogue no. L8880, ≥98%), L-α-phosphatidylcholine, (PC, Aladdin, catalogue no.
534 L130331, ≥99%), L-α-phosphatidylglycerol (PG, Aladdin, catalogue no. L130372;
535 ≥99%), L-α-phosphatidylethanolamine (PE, Aladdin, catalogue no. L130310; ≥99%) or
536 Cardiolipin (CL, Aladdin, catalogue no. B130227;≥99%) was loaded to the agar plate
537 that contains indicator strain. After the brevicidiene/cell membrane component
538 mixture solution drops had dried, the plates were transferred to a 37 °C incubator for
539 overnight incubation.

540 **Isothermal Titration Calorimetry (ITC) assay**

541 ITC was performed with the Low Volume NanoITC (TA Instruments) at 25°C to
542 determine the interaction between brevicidine and LPS, PG, or CL. Brevicidine was
543 diluted in a buffer (20 mM HEPES, pH7.0) to a final concentration of 50 μM. Samples
544 were degassed before use. The chamber was filled with 300 μL of the brevicidine
545 solution, and LPS (250μM), PG (500μM), or CL (500μM) was titrated into the
546 chamber at a rate of 1.96 μL/200 s with a stirring rate of 300 rpm. The control
547 experiment was performed with 20 mM HEPES titration to 50 μM brevicidine. The K_D
548 values of brevicidine to LPS, PG, or CL were calculated using the Nano Analyse
549 Software (Waters LLC).

550 **Transcriptome analysis of *E. coli* O101 treated with brevicidine**

551 Three replicates of overnight bacteria cultures were diluted at 1:100 in MHB and
552 grown at 37˚C with aeration at 220rpm. Bacteria were grown to an OD_{600} of 0.4, and
553 then the concentration of cells was adjusted to an OD_{600} of 0.2 in MHB. Subsequently,
554 the bacteria were treated with brevicidine at a final concentration of 0.5μM (0.8
555 mg/L). Bacteria without brevicidine treatment were used as untreated control. Three
556 replicates were performed for both brevicidine treated and untreated bacterial
557 cultures, 4ml for each sample. After incubation at 37˚C with aeration at 220rpm for
558 1h, the bacteria from different treatments were collected by centrifuging, and the
559 bacterial pallets were stored in liquid nitrogen immediately. Subsequently, the
560 samples were sent to Novogene Co., Ltd (China) for transcriptome analysis. After RNA
561 extraction, mRNA purification, and cDNA synthesis, the samples were sequenced on
562 the Illumina NovaSeq6000. The quality of the resulting fastq reads was mapped on
563 the reference genome using Bowtie2 2.3.4.3 using default settings. Feature Counts

564 1.5.0-p3 was used to get the gene counts. DESeq2 1.20 was used to identify all genes,
565 and padj ≤0.05 and |log2 (foldchange) | ≥ 0 of genes between two treatments were
566 regarded as differentially expressed genes (DEGs). The volcano map and KEGG
567 enrichment of DEGs were performed with Magic Novogene package
568 (https://magic.novogene.com). The RNA-Seq data have been deposited in the NCBI
569 Gene Expression Omnibus with the accession number PRJNA872022.

570 Mouse peritonitis–sepsis model

571 Brevicidine was tested against *E. coli* O101 in a mouse peritonitis–sepsis model to
572 assess its *in vivo* bioavailability. BALB/c male mice (n=6 per group) were infected with
573 0.4ml of bacterial suspension (2×10^9 c.f.u. per mouse) via intraperitoneal injection, a
574 concentration that achieves approximately 80% mortality within 48 h post-infection.
575 At 1h post-infection, mice were treated with 0.9% NaCl, brevicidine (40mg/kg),
576 brevicidine (20mg/kg), brevicidine (10mg/kg), or colistin (20mg/kg) via intravenous
577 injection. Mice without *E. coli* O101 infections were used as the normal group control.
578 Once the infected mice died, different organs, including the heart, liver, spleen, lung,
579 and kidney, were collected and homogenized in sterilized PBS for bacterial load
580 quantification. At 24h post-infection, the organs of the survived mice were collected
581 to measure the bacterial load. In addition, the same mouse peritonitis–sepsis model
582 was determined for 7d (n=10), and the bacterial load in the organs of surviving mice
583 was quantified at 7 days post-infection.

584 Statistical analysis

585 GraphPad Prism 8.0 was used to fit the data of Fig. 2, Fig. 3, Fig. 5, Fig. 8, and
586 Supplementary Fig. S1. The statistical significance of the data was assessed using a
587 two-tailed Student's t-test with GraphPad Prism 8.0. Correlation analyses were

evaluated by Pearson r2, ns: $p>0.05$, *$p<0.05$, **$p<0.01$, ***$p<0.001$, and ****$p<0.0001$.

Data Availability Statement: The transcriptome (RNA sequencing) data that support the findings of this study have been deposited in the NCBI Sequence Read Archive (SRA) with the accession code PRJNA872022.

Finding: Xinghong Zhao was supported by the Science and Technology Project of Sichuan Province (2022YFH0057). Hongping Wan was supported by the Science and Technology Project of Sichuan Province (2022YFH0062).

Competing Interests: The authors have declared that no competing interests exist.

Acknowledgments

We thank Prof. Kui Zhu (National Center for Veterinary Drug Safety Evaluation, College of Veterinary Medicine, China Agricultural University, Beijing, China.) for providing the multidrug resistant *Escherichia coli* (B2 and 16QD) strains.

602 ## References

603 1. O'neill, J. I. M. (2014) Antimicrobial resistance: tackling a crisis for the health
604 and wealth of nations. *Rev. Antimicrob. Resist.* **1**, 1–16
605 2. Kwon, J. H., and Powderly, W. G. (2021) The post-antibiotic era is here. *Science.*
606 **373**, 471
607 3. Knight, G. M., Glover, R. E., McQuaid, C. F., Olaru, I. D., Gallandat, K., Leclerc,
608 Q. J., Fuller, N. M., Willcocks, S. J., Hasan, R., and van Kleef, E. (2021)
609 Antimicrobial resistance and COVID-19: Intersections and implications. *Elife*.
610 **10**, e64139
611 4. Strathdee, S. A., Davies, S. C., and Marcelin, J. R. (2020) Confronting
612 antimicrobial resistance beyond the COVID-19 pandemic and the 2020 US
613 election. *Lancet*. **396**, 1050–1053
614 5. Lai, C.-C., Chen, S.-Y., Ko, W.-C., and Hsueh, P.-R. (2021) Increased
615 antimicrobial resistance during the COVID-19 pandemic. *Int. J. Antimicrob.*
616 *Agents*. **57**, 106324
617 6. Rizvi, S. G., and Ahammad, S. Z. (2022) COVID-19 and antimicrobial resistance:
618 A cross-study. *Sci. Total Environ.* **807**, 150873
619 7. Butler, M. S., Blaskovich, M. A. T., and Cooper, M. A. (2017) Antibiotics in the
620 clinical pipeline at the end of 2015. *J. Antibiot. (Tokyo).* **70**, 3
621 8. Butler, M. S., Blaskovich, M. A., and Cooper, M. A. (2013) Antibiotics in the
622 clinical pipeline in 2013. *J. Antibiot. (Tokyo).* **66**, 571
623 9. Roemer, T., and Boone, C. (2013) Systems-level antimicrobial drug and drug
624 synergy discovery. *Nat. Chem. Biol.* **9**, 222
625 10. Süssmuth, R. D., and Mainz, A. (2017) Nonribosomal peptide
626 synthesis—principles and prospects. *Angew. Chemie Int. Ed.* **56**, 3770–3821
627 11. Li, Y.-X., Zhong, Z., Zhang, W.-P., and Qian, P.-Y. (2018) Discovery of cationic
628 nonribosomal peptides as Gram-negative antibiotics through global genome
629 mining. *Nat. Commun.* **9**, 3273
630 12. Zhao, X., Li, Z., and Kuipers, O. P. (2020) Mimicry of a Non-ribosomally
631 Produced Antimicrobial, Brevicidine, by Ribosomal Synthesis and
632 Post-translational Modification. *Cell Chem. Biol.* **27**, 1262-1271.e4
633 13. Al Ayed, K., Ballantine, R. D., Hoekstra, M., Bann, S. J., Wesseling, C. M. J.,
634 Bakker, A. T., Zhong, Z., Li, Y.-X., Brüchle, N. C., and van der Stelt, M. (2022)
635 Synthetic studies with the brevicidine and laterocidine lipopeptide antibiotics
636 including analogues with enhanced properties and in vivo efficacy. *Chem. Sci.*
637 **13**, 3563–3570
638 14. Zhao, X., and Kuipers, O. P. (2021) BrevicidineB, a new member of the
639 brevicidine family, displays an extended target specificity. *Front. Microbiol.* **12**,
640 1482
641 15. Tacconelli, E., Magrini, N., Kahlmeter, G., and Singh, N. (2017) Global priority
642 list of antibiotic-resistant bacteria to guide research, discovery, and
643 development of new antibiotics. *World Heal. Organ.* **27**, 318–327
644 16. Song, M., Liu, Y., Huang, X., Ding, S., Wang, Y., Shen, J., and Zhu, K. (2020) A

645 broad-spectrum antibiotic adjuvant reverses multidrug-resistant
646 Gram-negative pathogens. *Nat. Microbiol.* **5**, 1040–1050
647 17. Liu, Y., Shi, L., Su, L., van der Mei, H. C., Jutte, P. C., Ren, Y., and Busscher, H. J.
648 (2019) Nanotechnology-based antimicrobials and delivery systems for
649 biofilm-infection control. *Chem. Soc. Rev.* **48**, 428–446
650 18. Sharma, G., Sharma, S., Sharma, P., Chandola, D., Dang, S., Gupta, S., and
651 Gabrani, R. (2016) Escherichia coli biofilm: development and therapeutic
652 strategies. *J. Appl. Microbiol.* **121**, 309–319
653 19. Haney, E. F., Trimble, M. J., and Hancock, R. E. W. (2021) Microtiter plate
654 assays to assess antibiofilm activity against bacteria. *Nat. Protoc.* **16**,
655 2615–2632
656 20. Zhao, X., Yin, Z., Breukink, E., Moll, G. N., and Kuipers, O. P. (2020) An
657 Engineered Double Lipid II Binding Motifs-Containing Activity against
658 Enterococcus faecium. *Antimicrob. Agents Chemother.* **64**, 1–12
659 21. Ling, L. L., Schneider, T., Peoples, A. J., Spoering, A. L., Engels, I., Conlon, B. P.,
660 Mueller, A., Schäberle, T. F., Hughes, D. E., and Epstein, S. (2015) A new
661 antibiotic kills pathogens without detectable resistance. *Nature*. **517**, 455
662 22. Helander, I. M., and Mattila-Sandholm, T. (2000) Fluorometric assessment of
663 Gram-negative bacterial permeabilization. *J. Appl. Microbiol.* **88**, 213–219
664 23. Cochrane, S. A., Findlay, B., Bakhtiary, A., Acedo, J. Z., Rodriguez-Lopez, E. M.,
665 Mercier, P., and Vederas, J. C. (2016) Antimicrobial lipopeptide tridecaptin A1
666 selectively binds to Gram-negative lipid II. *Proc. Natl. Acad. Sci.* **113**,
667 11561–11566
668 24. Stokes, J. M., Yang, K., Swanson, K., Jin, W., Cubillos-Ruiz, A., Donghia, N. M.,
669 MacNair, C. R., French, S., Carfrae, L. A., and Bloom-Ackerman, Z. (2020) A
670 deep learning approach to antibiotic discovery. *Cell*. **180**, 688–702
671 25. Ahmed, S., and Booth, I. R. (1983) The use of valinomycin, nigericin and
672 trichlorocarbanilide in control of the protonmotive force in Escherichia coli
673 cells. *Biochem. J.* **212**, 105–112
674 26. Bakker, E. P., and Mangerich, W. E. (1981) Interconversion of components of
675 the bacterial proton motive force by electrogenic potassium transport. *J.*
676 *Bacteriol.* **147**, 820–826
677 27. Malina, A., and Shai, Y. (2005) Conjugation of fatty acids with different lengths
678 modulates the antibacterial and antifungal activity of a cationic biologically
679 inactive peptide. *Biochem. J.* **390**, 695–702
680 28. Li, Y. X., Zhong, Z., Zhang, W. P., and Qian, P. Y. (2018) Discovery of cationic
681 nonribosomal peptides as Gram-negative antibiotics through global genome
682 mining. *Nat. Commun.* **9**, 2–10
683 29. Sohlenkamp, C., and Geiger, O. (2016) Bacterial membrane lipids: diversity in
684 structures and pathways. *FEMS Microbiol. Rev.* **40**, 133–159
685 30. Santos, R. S., Figueiredo, C., Azevedo, N. F., Braeckmans, K., and De Smedt, S.
686 C. (2018) Nanomaterials and molecular transporters to overcome the bacterial
687 envelope barrier: Towards advanced delivery of antibiotics. *Adv. Drug Deliv.*
688 *Rev.* **136**, 28–48

31. Wiegand, I., Hilpert, K., and Hancock, R. E. W. (2008) Agar and broth dilution methods to determine the minimal inhibitory concentration (MIC) of antimicrobial substances. *Nat. Protoc.* **3**, 163
32. Li, Z., Chakraborty, P., de Vries, R. H., Song, C., Zhao, X., Roelfes, G., Scheffers, D., and Kuipers, O. P. (2020) Characterization of two relacidines belonging to a novel class of circular lipopeptides that act against Gram-negative bacterial pathogens. *Environ. Microbiol.* **22**, 5125–5136
33. Li, Z., de Vries, R. H., Chakraborty, P., Song, C., Zhao, X., Scheffers, D.-J., Roelfes, G., and Kuipers, O. P. (2020) Novel modifications of nonribosomal peptides from Brevibacillus laterosporus MG64 and investigation of their mode of action. *Appl. Environ. Microbiol.*